SUPPORTING INFORMATION

Preparation and application of D-A conjugated electrochromic polymers with side chain carbazole active groups in supercapacitors

Pengna Wang [a], *Ying Sun* [a], *Jie Li* [a], *Weiwei Kang* [c], *Guanqun Zhu* [a], *Huijun Zhang* [a];

Xueqin Zhang [a], *Hong Yang* [a], *Bao-Ping Lin* * [a b]

a. School of Chemistry and Chemical Engineering, Southeast University, Nanjing 211189, China

b. School of Pharmaceutical and Chemical Engineering, Chengxian College, Southeast University, Nanjing 210088, China

c. College of Chemistry and Chemical Engineering, Henan Polytechnic University, Jiaozuo 454000, China

*Corresponding authors. E-mail addresses: lbp@seu.edu.cn

CONTENTS

1. Experimental details

Common chemicals and solvent such as 4-nitroaniline, sulfuric acid, iodine chloride, sodium nitrite, carbazole, anhydrous potassium carbonate, ketone iodide, 3, 5-diiodinitrobenzene, 18-crown ether-6, ethyl acetate, dichloromethane, n-hexane, ethanol in the synthesis process were purchased from well-known reagent companies such as Aladdin. The purity of the chemical is analytically pure. Dicyclopentadiene benzo thiophene (IDT66) and IDT69 were purchased from Derthon Optoelectronic Materials Science Technology Co. Ltd. The purity of the compound was 98%. Pd2$(dba)_3$, p$(o\text{-}tol)_3$ were purchased from Sigma-Aldrich. The purity of the compound was 99%. It should be noted that the solvents used in the polymerization process were either purchased at the anhydrous level or re-distilled by themselves. The propylene carbonate (PC) used in the electrochemical test was 99.5% pure, and the ITO conductive glass was purchased from Wuhan Geao Company with a thickness of 1.1 nm and a square resistance of 8 Ω.

Nuclear magnetic resonance spectroscopy (^{1}H NMR) was carried out by means of a nuclear magnetic resonance apparatus Burke 600 MHz, and deuterated chloroform ($CDCl_3$) or DMSO-d_6 was used as a solvent, TMS calibration. We used gaussview09 software to predict polymer molecules. The surface morphology of the polymer film was analyzed using the Scanning electron microscope of FEI Inspect F50. And the thermal stability of the polymer was obtained by a TG209F3 thermogravimetric

analyzer under the conditions of heating from room temperature to 800 °C at a heating rate of 10 °C min^{-1} under a nitrogen atmosphere. UV-vis absorption spectroscopy (UV-vis) was obtained using a UV-2450 UV spectrophotometer. The film sample was prepared by spraying the material onto the ITO glass. And the electrochromic pattern was obtained by the electrochemical workstation CHE660 in combination with UV-2450. In a 10*10*90 mm electrolyte cell, the constant voltage method was used in the electrochemical workstation to apply different voltages to the electrodes. At the same time, UV-2450 UV spectrophotometer was used to test the UV absorption peaks of the samples under different voltages. The electrochemical tests in this paper were obtained using Shanghai Chenhua CHI660 electrochemical workstation. While all the electrochemical tests were carried out under anhydrous and oxygen-free conditions. To exclude the influence of oxygen and moisture, nitrogen was propagated by nitrogen pack to the electrolyte for 1 hour prior to testing. This paper uses a three-electrode system to characterize the basic electrochemical performance of the prepared polymer electrode. In the three-electrode test, an Ag/Ag^{+} electrode was used as the reference electrode, a 1×2 platinum electrode was used as the counter electrode, and the polymer electrode or oxide electrode was used as the working electrode. The electrolyte is 0.5 M $LiClO_4$/PC solution.

2. Experimental section

2.1 Electrodes Preparation and characterization

The polymer electrode was prepared by the spraying method of polymer solution. The polymer was dissolved in chloroform at a concentration of 10 mg mL^{-1}. In order

to prevent particles from clogging the nozzle, an organic filter with a pore size of 0.22 μm was used to filter the solution again. The pre-treated ITO glass (the glass is coated with indium tin oxide, width 10mm, length 20mm, thickness 0.7mm; surface resistivity: 8 Ω) is on the heating plate (50 ℃). And then fix the ITO glass sheet on the hot stage. The substrate temperature (50 ℃), air flow pressure (150 Pa), spraying angle (45 °) and spraying distance (10 cm) are kept constant. Four consecutive layers are deposited with 100 s break between sequences as previously optimized. The ITO electrode was cured by heating at 50 °C for 20 minutes. In this way, the load of active material on the ITO glass can be kept stable every time.[1-4]

2.2 Synthesis of compounds

The experimental route: In a 100 ml single port flask, 4-nitroaniline (3.33 g) was dissolved in 10% H_2SO_4 (40 ml), and then ICl (10 g) was added slowly to react at 80 ℃ for 8 h. After the reaction was completed, the reaction liquid was cooled to room temperature, and yellow solid precipitated. **2,6-diiodio-4-nitroaniline**(8.289 g) was obtained by suction filtration. The yield was 89.0%.[5-6] ^{1}H NMR (600 MHz, DMSO-d_6, δ, ppm): 8.446(s, 2H, Ar-H), 6.362(s, 2H, N-H). ^{13}C NMR (151 MHz, DMSO-d_6) δ: 153.659, 138.037, 135.272, 78.998. EI-MS: Calcd. for $C_6H_4I_2N_2O_2$, 389.84; Found: 390.721 $[M+1]^+$.

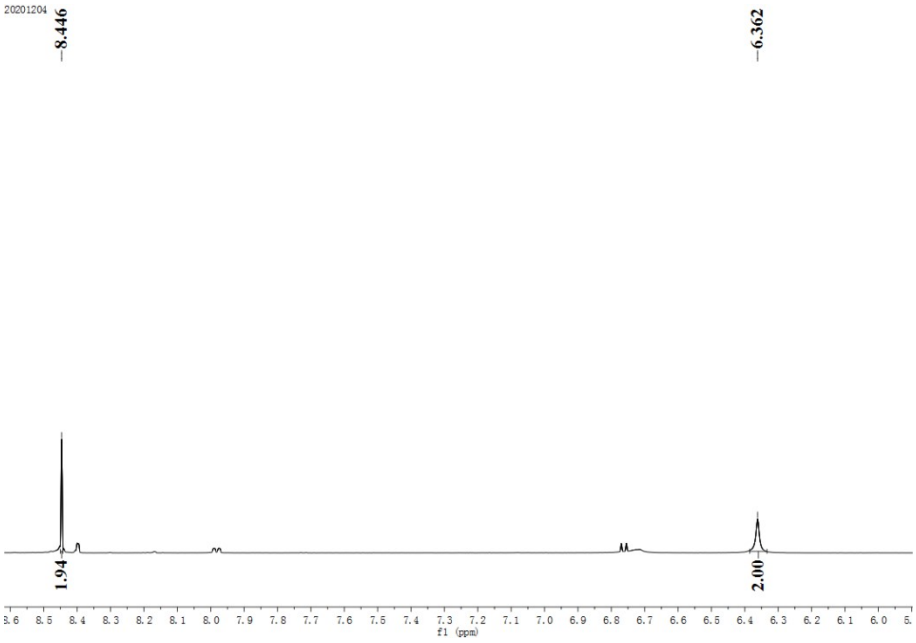

Figure S1 ^{1}H NMR spectrum of 2,6-diiodio-4-nitroaniline.

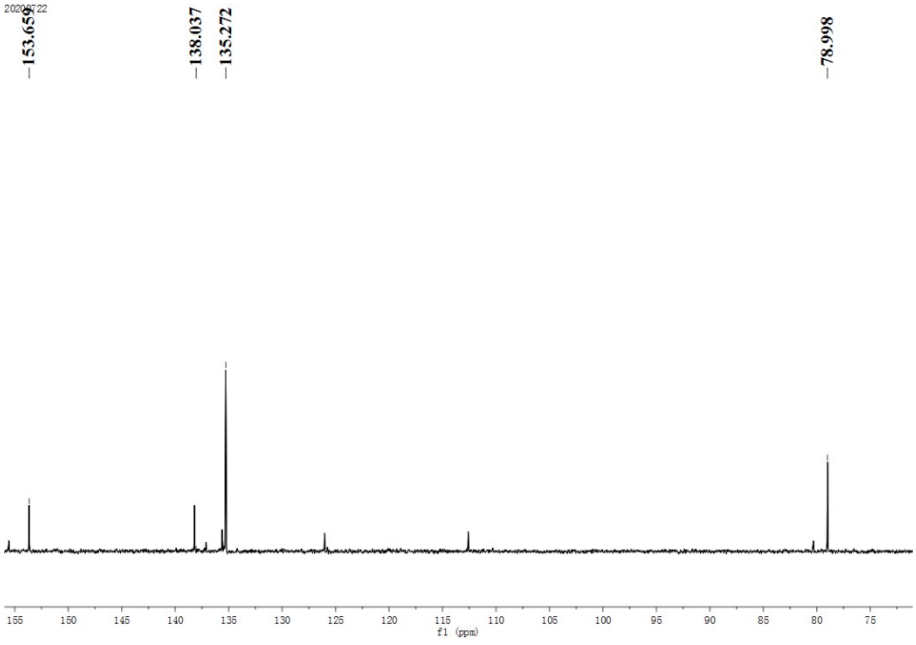

Figure S2 ^{13}C NMR spectrum of 2,6-diiodio-4-nitroaniline.

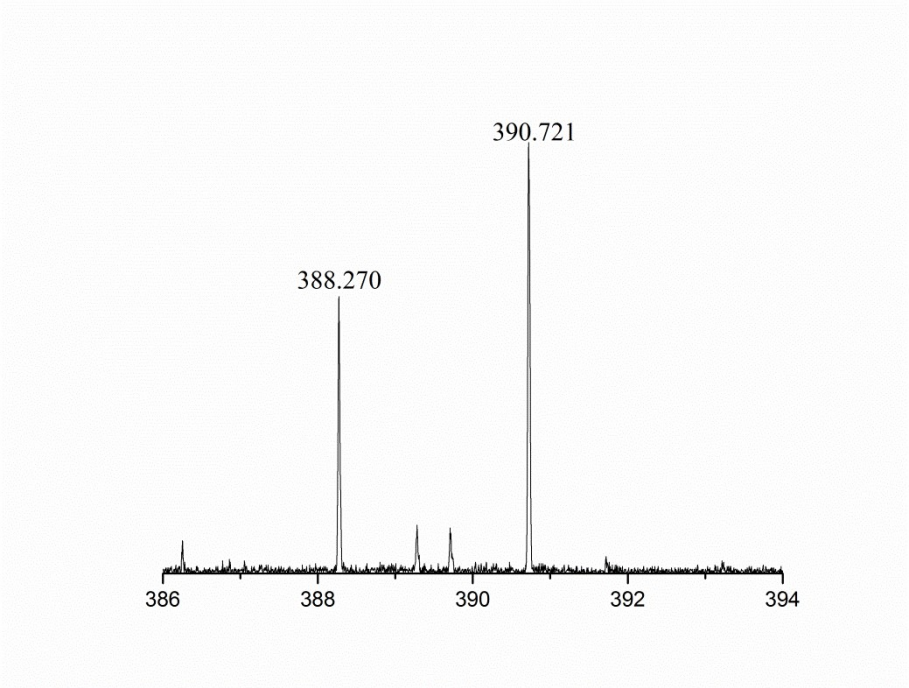

Figure S3 Mass spectrometry of 2,6-diiodio-4-nitroaniline.

98% H_2SO_4 (40 ml) was slowly added into a 100 ml three port flask, kept at 0 ℃, and then 2,6-diiodo-4-nitroaniline (3.567 g, 9.15 mmol) was slowly added into the three necked flask and stirred for 1 h. Sodium nitrite (1.452 g, 21.05 mmol) was added into the reaction solution and stirred for 2 h in ice bath. Ice water (20 mL) was added to the reaction solution. The mixture was then partially added to the boiling copper sulfate ethanol solution and reacted for 2 h.[7] The crude product was purified by column chromatography to obtain **3, 5-diiodinitrobenzene** (2.813 g, 90.0%). ^{1}H NMR (600 MHz, $CDCl_3$, δ, ppm): 8.517-8.519(d, J =1.2 Hz, 2H, Ar-H), 8.370-8.375(t, J =3 Hz, 1H, Ar-H). ^{13}C NMR (151 MHz, $CDCl_3$) δ: 149.976, 147.492, 130.809, 93.117. EI-MS: Calcd. for $C_6H_3I_2NO_2$, 374.83; Found: 374.881 $[M+1]^+$.

Figure S4 ^{1}H NMR spectrum of 3, 5-diiodinitrobenzene.

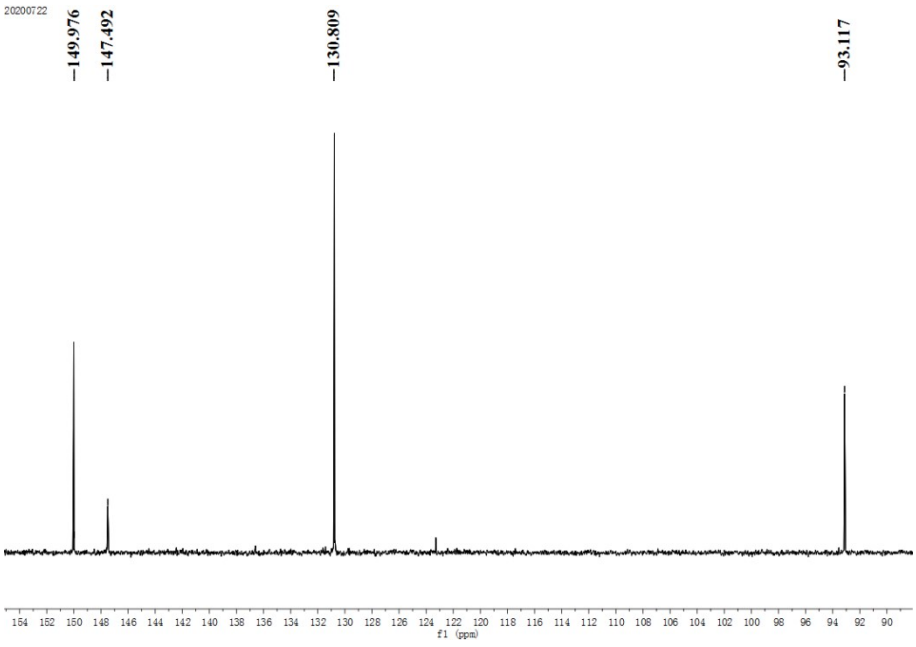

Figure S5 ^{13}C NMR spectrum of 3, 5-diiodinitrobenzene.

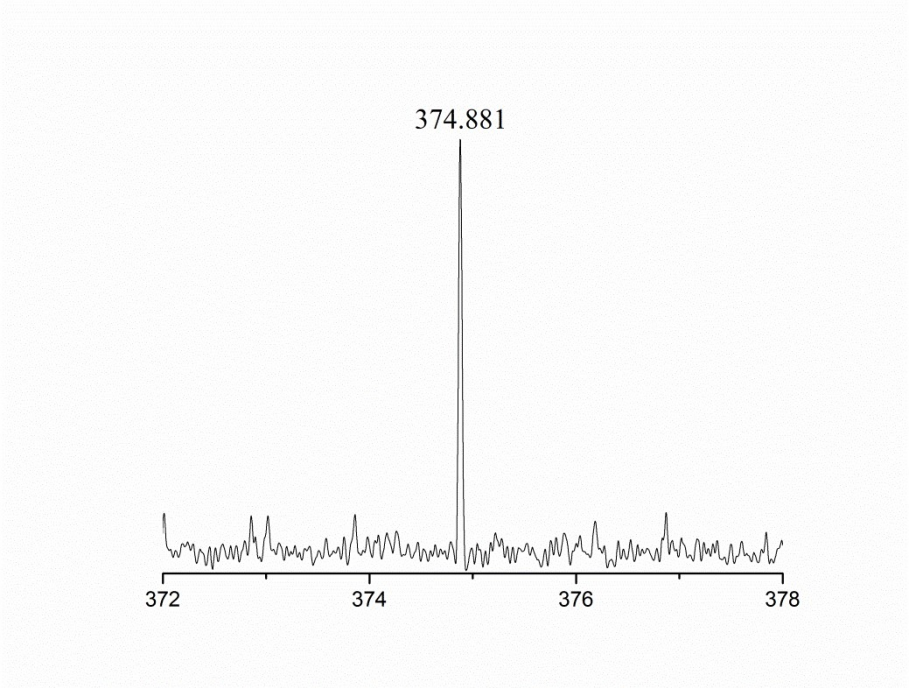

Figure S6 Mass spectrometry of 3, 5-diiodinitrobenzene.

An anhydrous DMF 100 mL, carbazole (9.8 g, 58.7 mmol), anhydrous potassium carbonate (8.1 g, 58.7 mmol), ketone iodide (11.2 g, 58.7 mmol) and 18-crown ether-6 (1.4 g, 5.3 mmol) were added into a 2500 ml three port flask and stirred for 1 h. Then 3, 5-diiodinitrobenzene (10.0 g, 26.7 mmol) was added under nitrogen protection at 150 ℃ for 24 h. The reaction liquid was cooled to room temperature and poured into water (1000 mL) to filter the crude product. The crude product was purified by column chromatography (dichloromethane / n-hexane =1/4). The obtained yellow solid (10 g, 22 mmol) was added to a three-bottle flask containing 500 mL anhydrous ethanol, followed by Pd/C (0.2 g) and 60 mL hydrazine hydrate, which was reacted at 80 ℃ for 6 h. After the reaction, the filtrate was filtered at high temperature, and **3,5-di (9h-carbazol-9-yl) aniline** was obtained by recrystallization after vacuum distillation.[8] ^{1}H NMR (600 MHz, DMSO-d_6, δ, ppm): 8.238-8.250(d, J =7.2 Hz, 4H, Ar-H), 7.609-7.596(d, J =7.8 Hz, 4H, Ar-H), 7.490-7.465(t, J =15 Hz, 4H, Ar-H),

7.305-7.281(t, J =14.4 Hz, 4H, Ar-H), 6.950(s, 2H, Ar-H), 6.868(s, 1H, Ar-H), 5.902(s, 2H, N-H); ^{13}C NMR (151 MHz, DMSO-d_6) δ: 153.361, 140.456, 139.335, 126.75, 123.236, 120.992, 120.498, 111.247, 110.989, 110.470. EI-MS: Calcd. for $C_{30}H_{21}N_3$, 423.17; Found: 423.17 $[M+1]^+$.

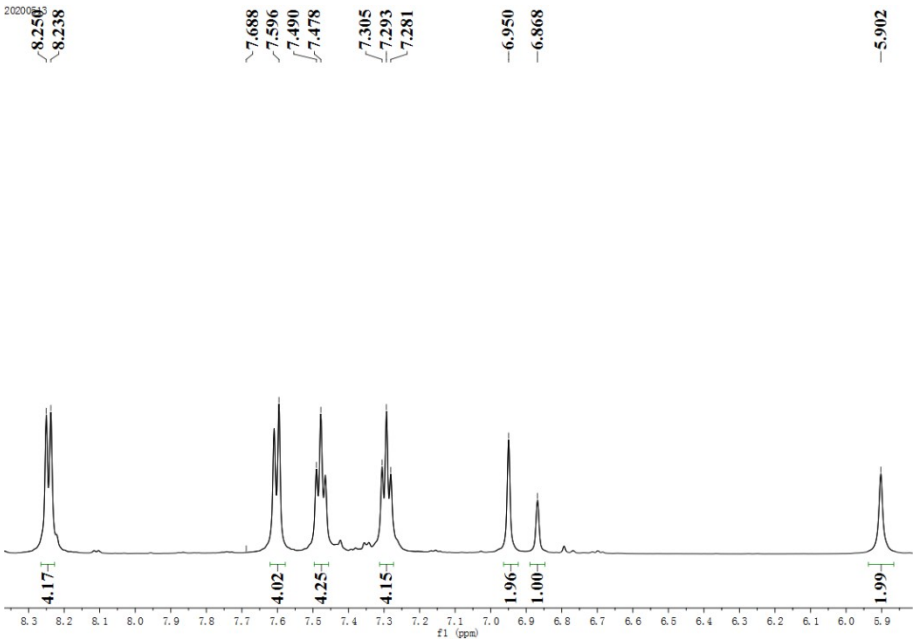

Figure S7 ^{1}H NMR spectrum of 3,5-di (9h-carbazol-9-yl) aniline.

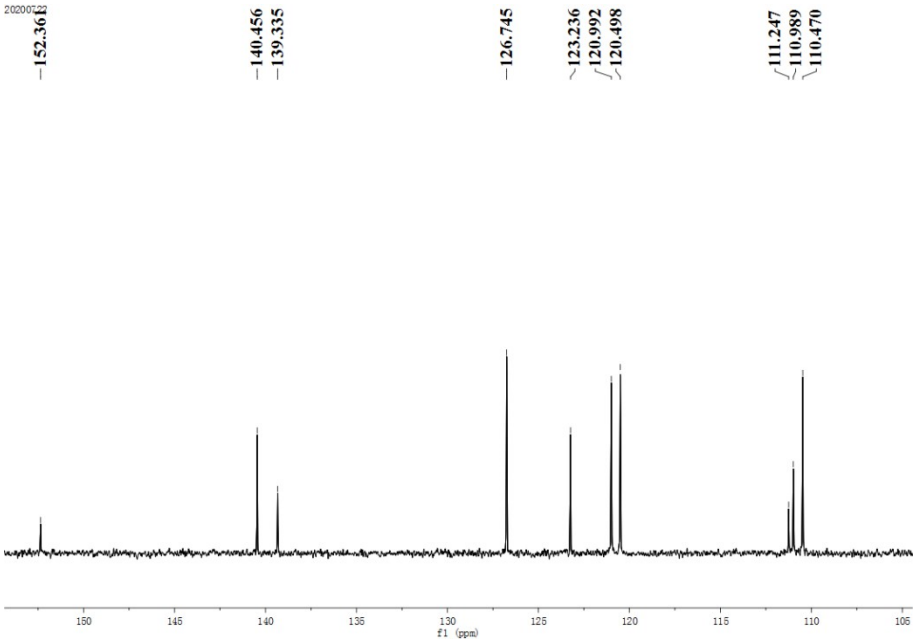

Figure S 8 ^{13}C NMR spectrum of 3,5-di (9h-carbazol-9-yl) aniline.

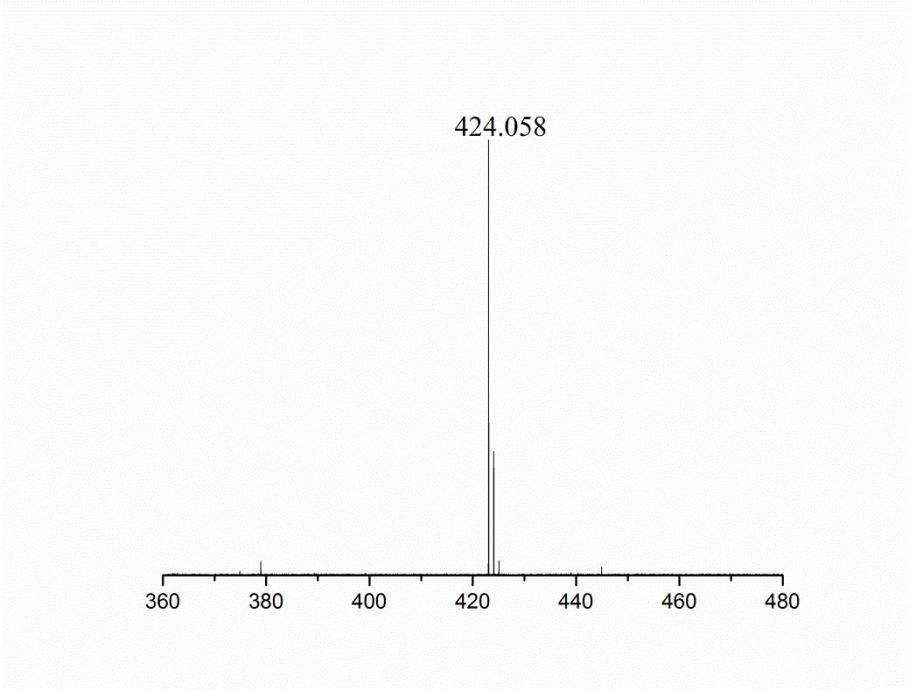

Figure S 9 Mass spectrometry of 3,5-di (9h-carbazol-9-yl) aniline.

3,5-bis(3,6-di-tert-butyl-9H-carbazol-9-yl)aniline ^{1}H NMR (600 MHz, DMSO-d_6, δ, ppm): 8.280(s, 4H, Ar-H), 7.510-7.516(t, J =3.6 Hz, 8H, Ar-H), 6.886-6.889(d, J =1.8 Hz, 2H, Ar-H), 6.834-6.839(t, J =3 Hz, 1H, Ar-H), 5.799-5.801(d, J =1.2 Hz, 2H, N-H), 1.417(s, 36H, C-H). ^{13}C NMR (151 MHz, DMSO-d_6) δ: 142.935, 139.727, 138.841, 124.212, 123.355, 117.079, 110.515, 110.163, 109.914, 34.969, 32.304. EI-MS: Calcd. for $C_{46}H_{53}N_3$, 647.42; Found: 647.363 $[M]^+$.

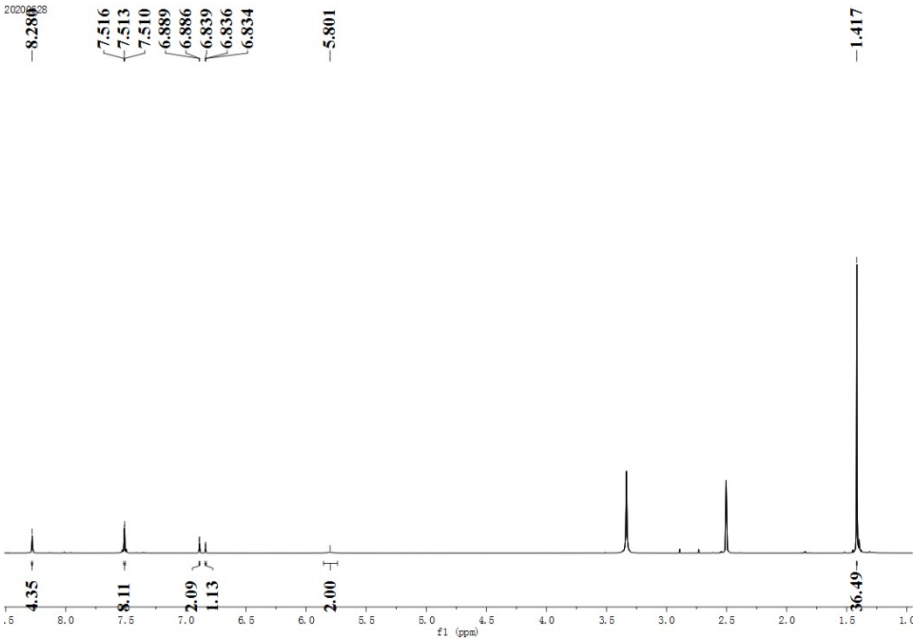

Figure S10 ^{1}H NMR spectrum of 3,5-bis(3,6-di-tert-butyl-9H-carbazol-9-yl)aniline.

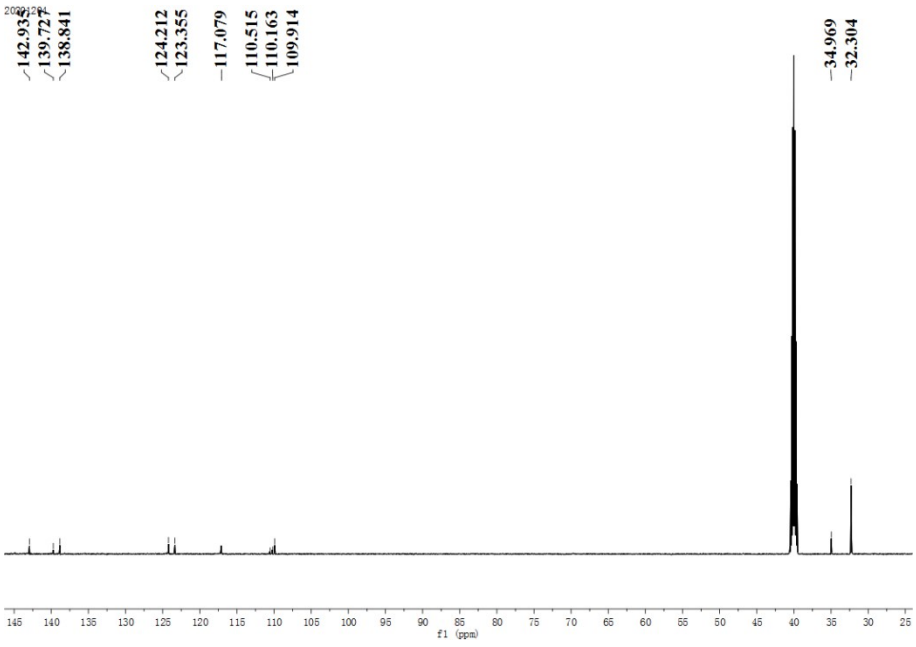

Figure S11 ^{13}C NMR spectrum of 3,5-bis(3,6-di-tert-butyl-9H-carbazol-9-yl)aniline.

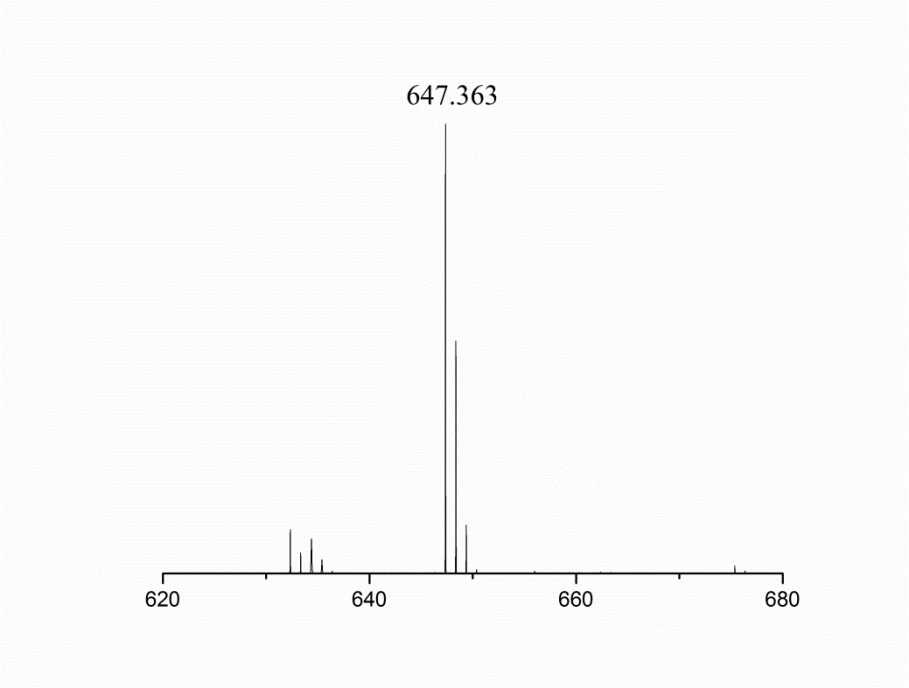

Figure S12 Mass spectrometry of 3,5-bis(3,6-di-tert-butyl-9H-carbazol-9-yl)aniline.

First, 19 ml toluene, 3.9 ml DMF and a drop of triethylamine were mixed evenly to obtain the mixed solvent. 3,5-di (9h-carbazol-9-yl) aniline (0.42 g, 1.00 mmol) and 4,7-dibromoisobenzofuran-1,3-dione (0.30 g, 1.00 mmol) were added into the single-mouth flask, followed by the mixed solvent (6.5 mL). The mixture was refluxed at 110 ℃ under nitrogen protection for 12 h. After the reaction, the mixture was cooled to room temperature, and then poured into ethanol (15 ml) to obtain a yellow-brown precipitate. The solid was filtered and dried in vacuum. **4,7-dibromo-2-(3,5-di(9H-carbazol-9-yl)phenyl)-1H-indene-1,3(2H)-dione**（0.31 g, 74%） was obtained by column chromatography. ^{1}H NMR (600 MHz, $CDCl_3$, δ, ppm): 8.146-8.159(d, J =7.8 Hz, 4H, Ar-H), 7.917-7.922(t, J =3 Hz, 1H, Ar-H), 7.852-7.859(t, J =4.2 Hz, 2H, Ar-H), 7.773(s, 2H, Ar-H), 7.678-7.692(d, J =8.4 Hz, 4H, Ar-H), 7.499-7.474(t, J = 15 Hz, 4H, Ar-H), 7.343-7.318(t, J = 18 Hz, 4H, Ar-H). ^{13}C NMR (151 MHz, $CDCl_3$) δ: 139.277, 138.821, 125.420, 123.014, 122.794, 122.067, 119.608, 119.444, 108.804.

EI-MS: Calcd. for $C_{38}H_{21}BrN_3O_2$, 709.00; Found: 711.598 $[M+1]^+$.

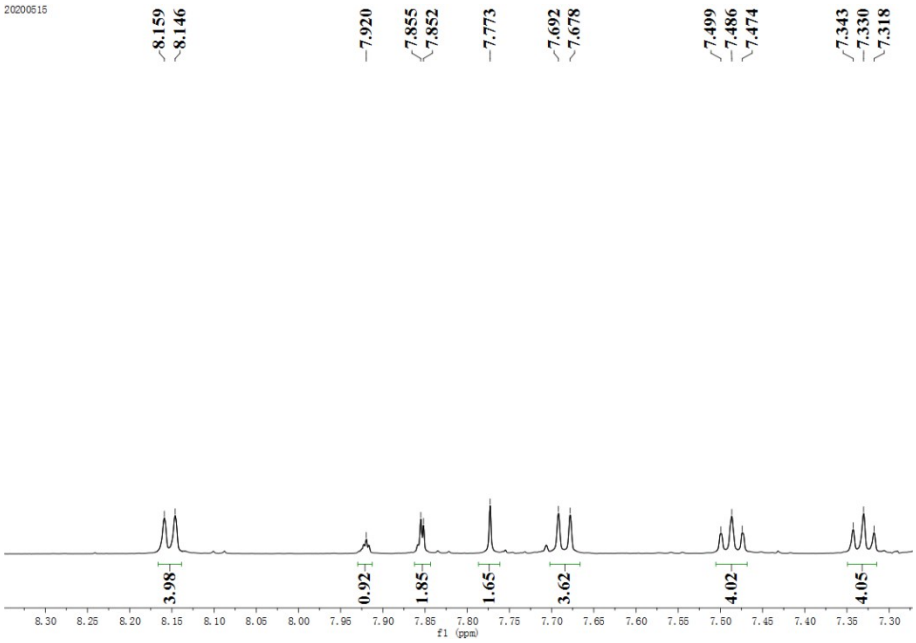

Figure S13 ^{1}H NMR spectrum of 4,7-dibromo-2-(3,5-di(9H-carbazol-9-yl)phenyl)-1H-indene-1,3(2H)-dione.

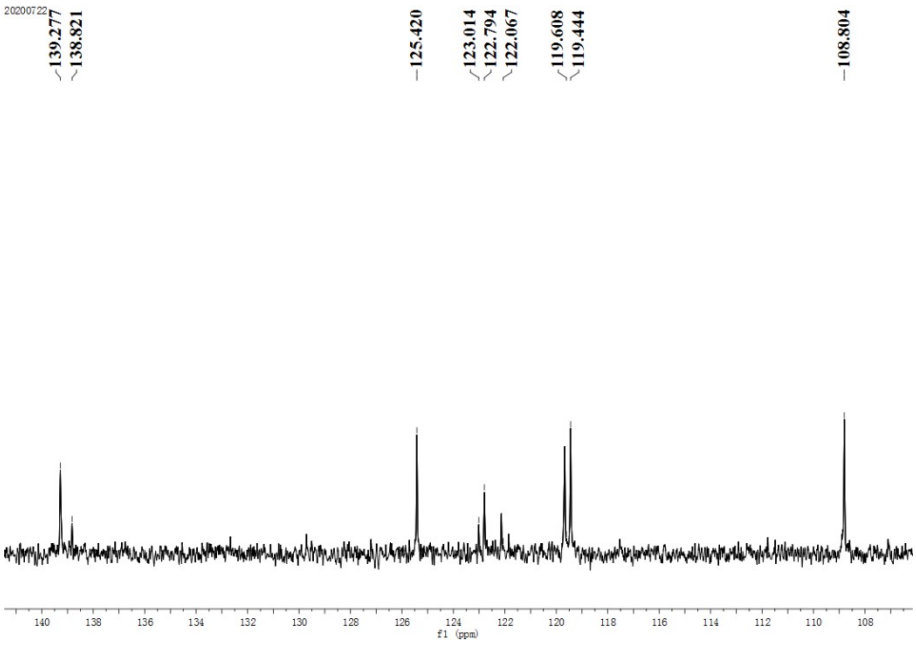

Figure S14 ^{13}C NMR spectrum of 4,7-dibromo-2-(3,5-di(9H-carbazol-9-yl)phenyl)-1H-indene-1,3(2H)-dione.

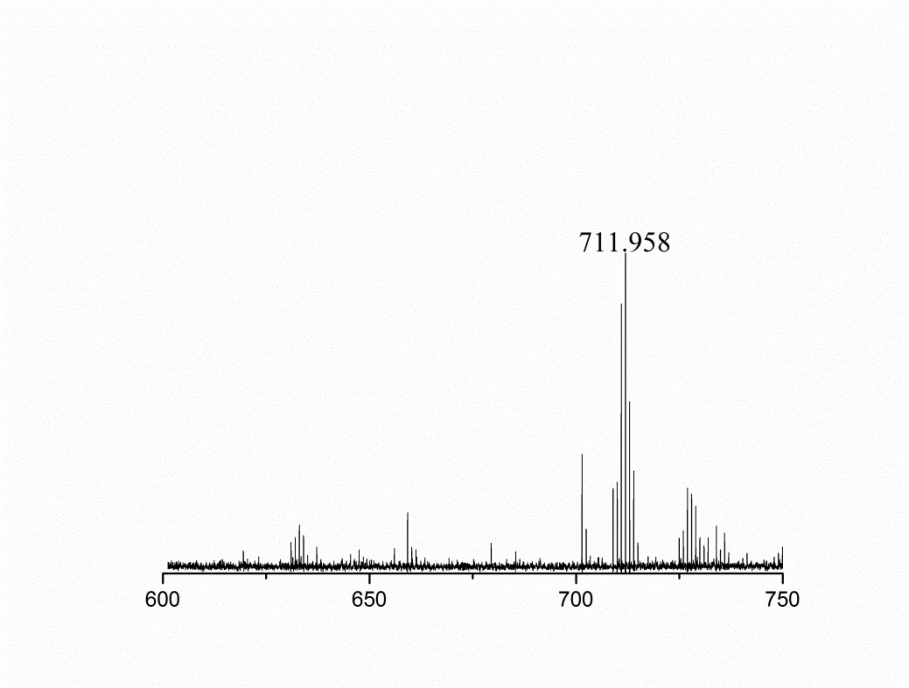

Figure S15 Mass spectrometry of 4,7-dibromo-2-(3,5-di(9H-carbazol-9-yl)phenyl)-1H-indene-1,3(2H)-dione.

2-(3,5-bis(3,6-di-tert-butyl-9H-carbazol-9-yl)phenyl)-4,7-dibromoisoindoline-1,3-dione ^{1}H NMR (600 MHz, $CDCl_3$, δ, ppm): 8.142(s, 2H, Ar-H), 8.139(s, 1H, Ar-H), 8.021(s, 2H, Ar-H), 7.895-7.901(t, J =3.6 Hz, 1H, Ar-H), 7.780-7.783(d, J =1.8 Hz, 2H, Ar-H), 7.766(s, 1H, Ar-H), 7.630(s, 1H, Ar-H), 7.626(s, 1H, Ar-H), 7.616(s, 1H, Ar-H), 7.535-7.538(d, J =1.8 Hz, 1H, Ar-H), 7.521-7.524(d, J =1.8 Hz, 2H, Ar-H), 1.470(s, 36H, C-H). ^{13}C NMR (151 MHz, $CDCl_3$) δ: 162.073, 142.692, 138.953, 137.332, 123.117, 122.471, 121.941, 120.729, 117.552, 115.188, 108.250, 33.794, 30.817, 28.675. EI-MS: Calcd. for $C_{54}H_{53}Br_2N_3O_2$, 933.25; Found: 935.273 $[M+1]^+$.

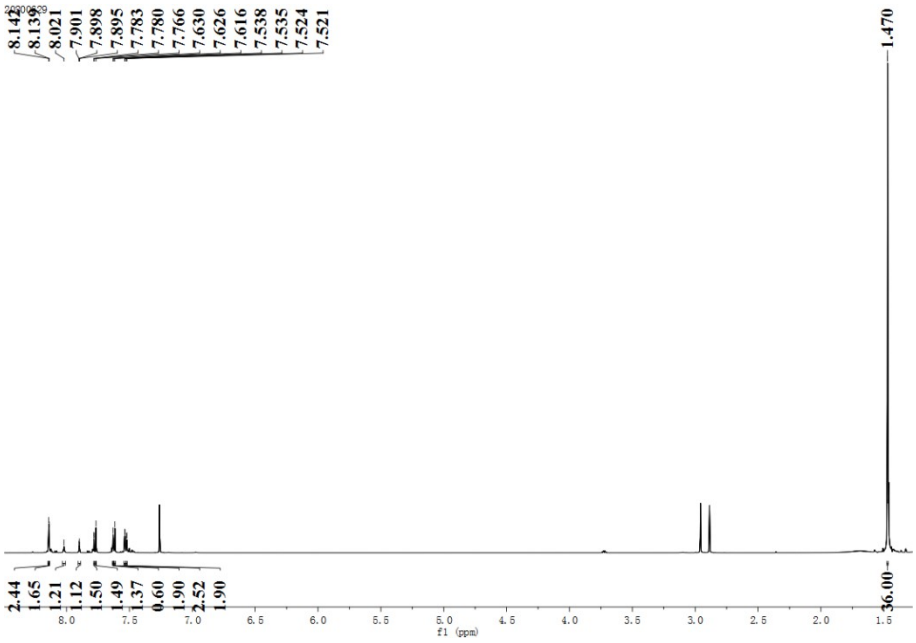

Figure S16 ^{1}H NMR spectrum of 2-(3,5-bis(3,6-di-tert-butyl-9H-carbazol-9-yl)phenyl)-4,7-dibromoisoindoline-1,3-dione.

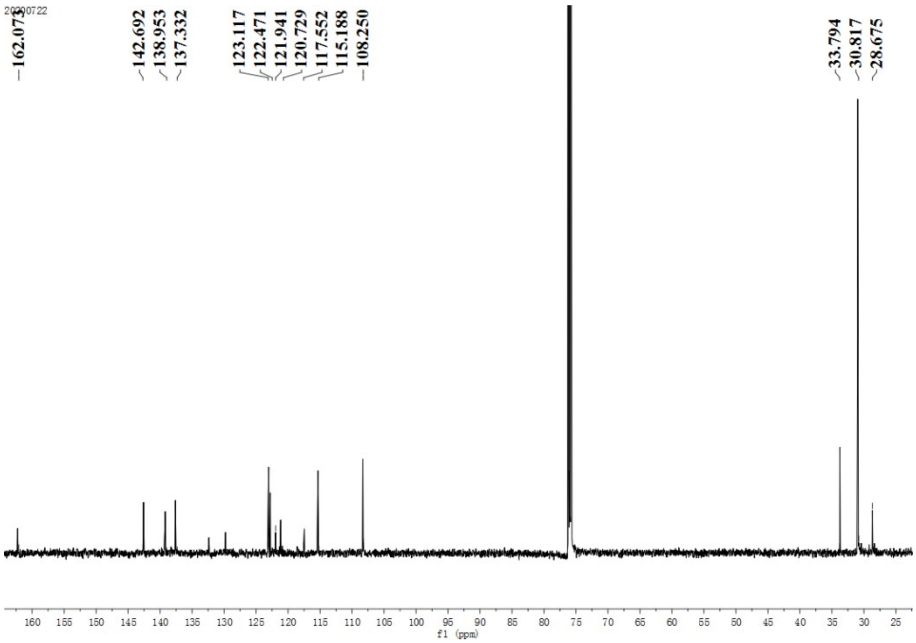

Figure S17 ^{13}C NMR spectrum of 2-(3,5-bis(3,6-di-tert-butyl-9H-carbazol-9-yl)phenyl)-4,7-dibromoisoindoline-1,3-dione.

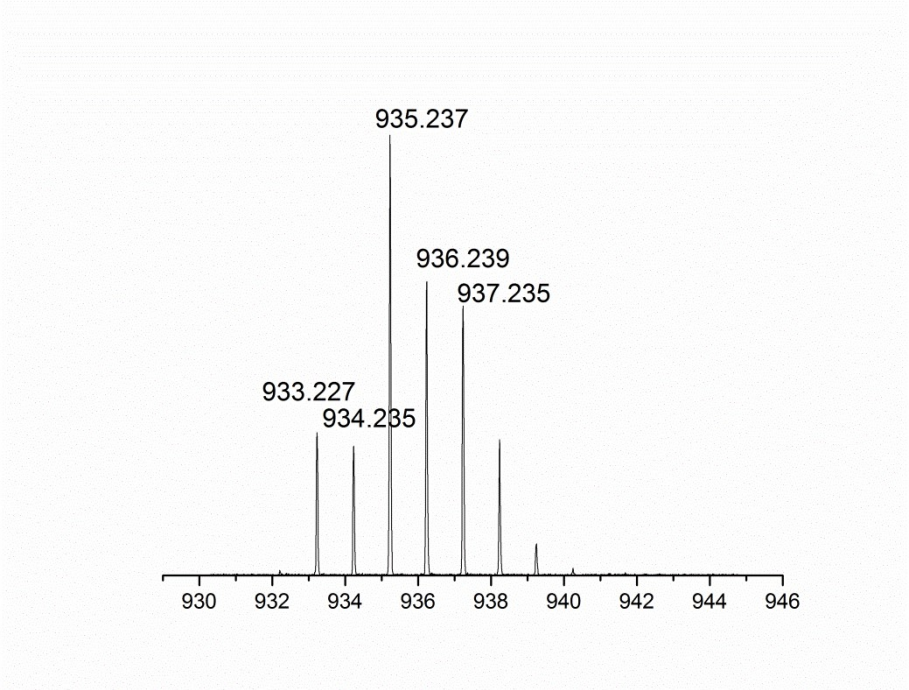

Figure S18 Mass spectrometry of 2-(3,5-bis(3,6-di-tert-butyl-9H-carbazol-9-yl)phenyl)-4,7-dibromoisoindoline-1,3-dione.

4,7-dibromo-2-(3,5-di(9h-carbazol-9-yl) phenyl)-1h-indene-e-1,3(2H)-dione (0.0709g, 0.1mmol) and dicyclopentadiene benzothiophene (IDT66) (0.1233 mg, 0.1 mmol) were added to the flask. The mixture of anhydrous toluene (4 ml) and anhydrous DMF (0.4 ml) were then added. After the solution was deoxidized by nitrogen, $Pd_2(dba)_3$ (4 mg) and P (o-tol)$_3$ (10 mg) were added quickly, and the solution was deoxidized again. The mixture was heated for 40 hours at the temperature of 120 ℃ and then dissolved in magneton-stirred methanol solution drop by drop. The precipitation was filtrated and collected. Acetone and n-hexane were used as solvents for each extraction for 12 h. Chloroform was then used to dissolve the solids again by dropping them into methanol. The polymer **PI-1** was obtained after vacuum drying. The synthesis methods of **PI-2**, **PI-3** and **PI-4** refer to **PI-1**.

PI-1 ^{1}H NMR (600 MHz, $CDCl_3$, δ, ppm): 8.329 (s, 2H, Ar-H), 8.138-8.150(d, J =7.2 Hz, 4H, Ar-H), 7.838-7.907(t, J =41.1 Hz, 4H, Ar-H), 7.666-7.679(d, J =7.8 Hz,

3H, Ar-H), 7.543(s, 2H, Ar-H), 7.448-7.472(t, J =14.4 Hz, 4H, Ar-H), 7.305-7.329(t, J =14.4 Hz, 4H, Ar-H), 7.209-7.221(d, J =14.4 Hz, 8H, Ar-H), 7.103-7.114(d, J =6.6 Hz, 8H, Ar-H), 2.556(s, 2H, C-H), 1.572(S, 20H, C-H), 1.275(s, 20H, C-H), 0.858(s, 12H, C-H). UV-vis($CHCl_3$):

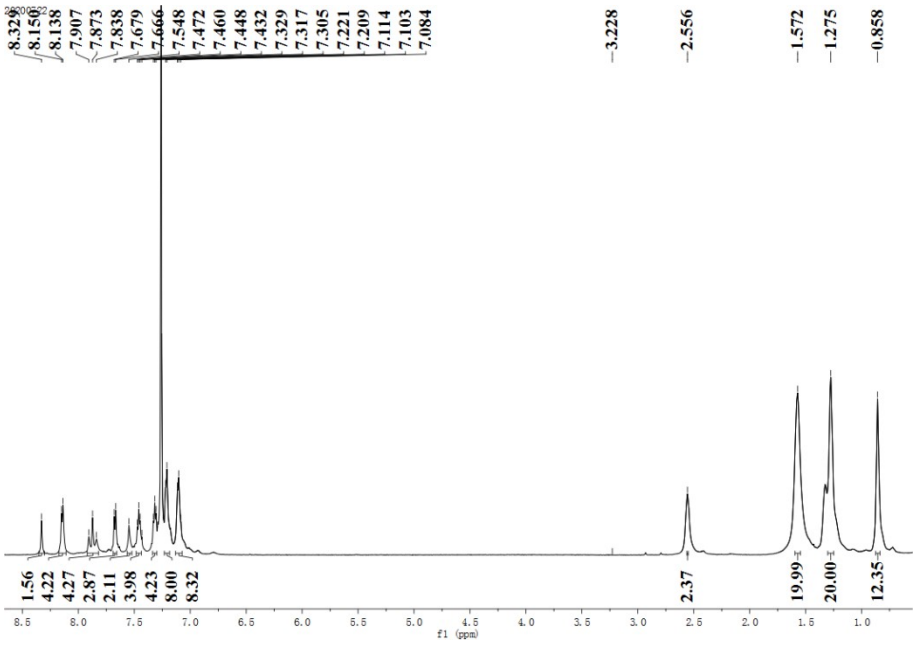

Figure S19 ^{1}H NMR spectrum of PI-1.

PI-2 ^{1}H NMR (600 MHz, $CDCl_3$, δ, ppm): 8.143-8.155(d, J =7.2 Hz, 4H, Ar-H), 7.827-7.907(m, J =48 Hz, 4H, Ar-H), 7.776-7.827(d, J =30.6 Hz, 2H, Ar-H), 7.663-7.727(m, J =38.4 Hz ,4H , Ar-H), 7.520(s, 1H, Ar-H), 7.438-7.455(t, J =10.2 Hz, 2H, Ar-H), 7.379-7.404(t, J =15.0 Hz, 4H, Ar-H), 7.292-7.315(t, J =13.8 Hz , 4H, Ar-H), 7.239(s, 4H, Ar-H), 6.966-7.082(m, J =69.6 Hz, 8H, C-H), 2.513(S, 2H, C-H), 1.571(S, 20H, C-H), 1.245-1.279(t, J =20.4 Hz, 20H, C-H), 0.836(s, 12H, C-H).

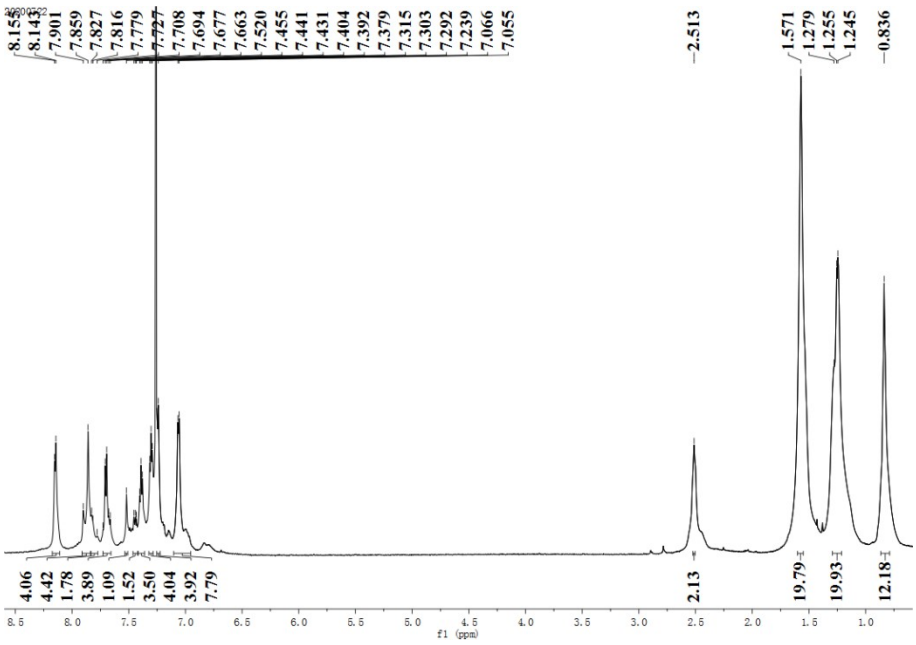

Figure S20 ^{1}H NMR spectrum of PI-2.

PI-3 ^{1}H NMR (600 MHz, $CDCl_3$, δ, ppm): 8.133(s, 4H, Ar-H), 7.895-7.907(d, J =7.2 Hz, 3H, Ar-H), 7.816-7.826(d, J =6 Hz, 3H, Ar-H), 7.751-7.767(d, J =9.6 Hz, 3H, Ar-H), 7.642(s, 2H, Ar-H), 7.628(s, 3H, Ar-H), 7.538(s, 2H, Ar-H), 7.451(s, 2H, Ar-H), 7.437(s, 2H, Ar-H), 7.431(s, 2H, Ar-H), 7.032(s, 2H, Ar-H), 7.072(s, 4H, Ar-H), 7.059(s, 6H, Ar-H), 2.495(s, 2H, C-H), 1.543(s, 36H, C-H), 1.446(s, 20H, C-H), 1.254(s, 20H, C-H), 0.802-0.823(t, J =12.6 Hz, 12H, C-H).

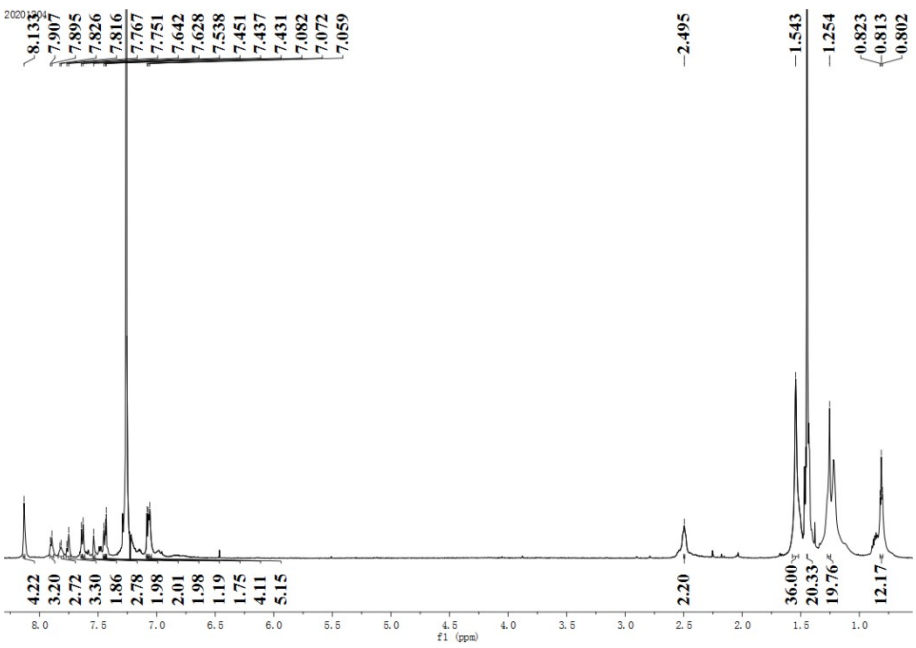

Figure S21 ^{1}H NMR spectrum of PI-3.

PI-4 ^{1}H NMR (600 MHz, $CDCl_3$, δ, ppm): 8.287(s, 1H, Ar-H), 8.054(s, 4H, Ar-H), 7.304(s, 1H, Ar-H), 7.749-7.753(d, J =2.4 Hz, 1H, Ar-H), 7.690-7.706(d, J =9.6 Hz, 2H, Ar-H), 7.519(s, 1H, Ar-H), 7.505(s, 2H, Ar-H), 7.481(s, 1H, Ar-H), 7.419-7.432(d, J =7.8 Hz, 4H, Ar-H), 7.221(s, 2H, Ar-H), 7.130-7.152(t, J =13.2 Hz, 6H, Ar-H), 7.097-7.110(m, J =7.8 Hz, 3H, Ar-H), 7.022-7.045(t, J =13.8 Hz, 8H, Ar-H), 2.483(s, 2H, C-H), 1.491(s, 36H, C-H), 1.374(s, 20H, C-H), 1.187-1.203(t, J =9.6 Hz, 20H, C-H), 0.771-0.789(t, J =10.8 Hz, 12H, C-H).

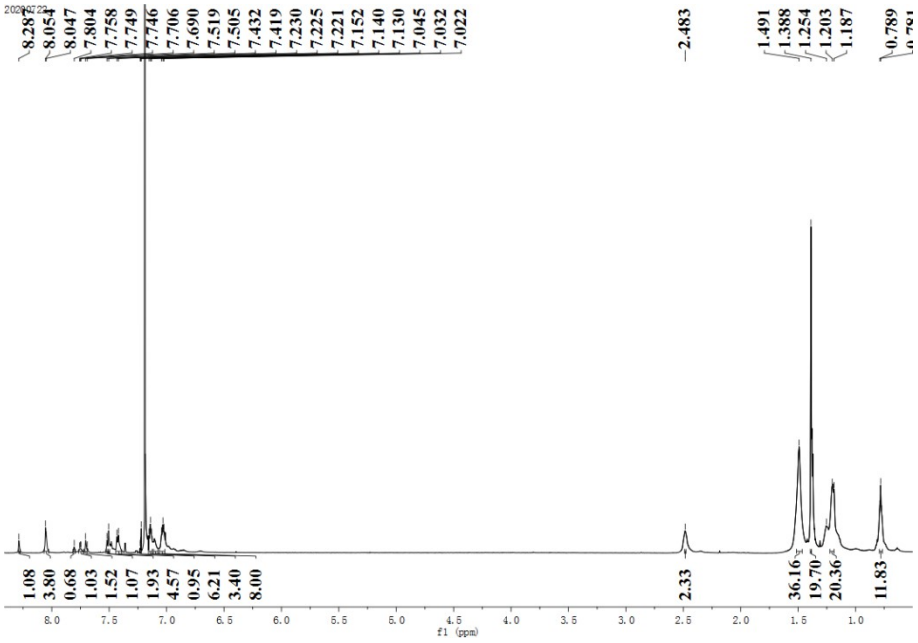

Figure S22 ^{1}H NMR spectrum of PI-4.

3. Determination of voltage window

Four polymer electrodes tested the properties under different voltage windows. The study showed that when the voltage window is greater than 0.9 v, the electrode will undergo obvious over-oxidation and affect the electrochemical performance of the electrode, so the voltage window is set to 0.9 v. However, the highest voltage tested for electrochromic properties is 1.6 v. This is because the discoloration can only be completed when the voltage is large enough.

4. Thermal properties

As shown in Figure S23, a thermogravimetric analyser (TGA) was used to probe the thermal transitions of compounds PI-1, PI-2, PI-3 and PI-4. For compounds PI-1, PI-2, PI-3 and PI-4, the decomposition temperatures are all relatively similar. All compounds exhibited excellent structural integrity in N_2, and the temperature at 5% weight loss was above 446 ℃, which was essentially due to the thermal

decomposition of the lateral chain of the overhanging structure of the polymer. Compared with that of PI-1, the TGA of PI-2 displayed an improved thermal firmness because the coplanarity of PI-2 is better than that of the other polymers, and the internal combination of molecules became firmer as the decomposition temperature increased. The increase in side-chain alkyl substituents increases the steric hindrance and reduces the molecular weight of the polymer, thus reducing the decomposition temperature.

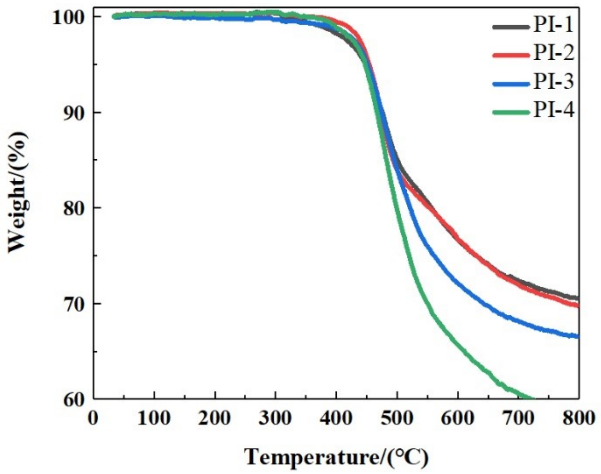

Figure S23 TGA curves of polymers in flowing nitrogen from 20 °C to 800 °C.

5. Surface morphology

Photos of the four polymer electrodes PI-1, PI-2, PI-3 and PI-4 are displayed in Figure S2 (a) and (d), respectively. The films exhibited a microphase-separated structure with many continuous channels. To examine the crossing point properties of the four electrodes, cross-sectional FE-SEM photographs of the PI-1, PI-2, PI-3 and PI-4 electrodes are examined, as shown in Figure S24(a) and (d), respectively. The polymer film and ITO glass are tightly bound. The cross section of the film also presents the structure of microphase separation. Hence, the polymer films could be

expected to facilitate ion diffusion.

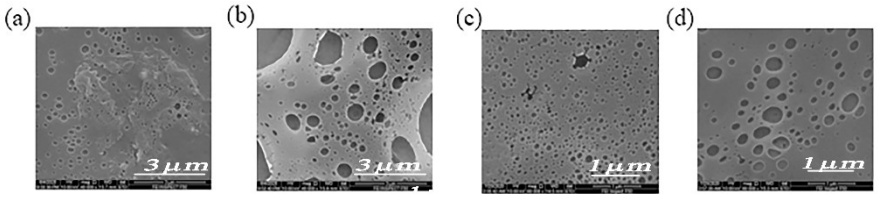

Figure S24 FE-SEM images of the (a) PI-1, (b) PI-2, (c) PI-3, and (d) PI-4 electrodes

The films exhibited micro-phase separated structure with many continuous channels. For the sake of examine the crossing point properties of the four electrodes, the cross-sectional FE-SEM photographs of the electrodes of PI-1, PI-2, PI-3 and PI-4 are examined, as shown in Figure S25 (a) and (d), respectively. The polymer film and ITO glass are tightly bound. The cross section of the film also presents the structure of microphase separation. Hence, the polymer films could be expected to facilitate the ion diffusion.

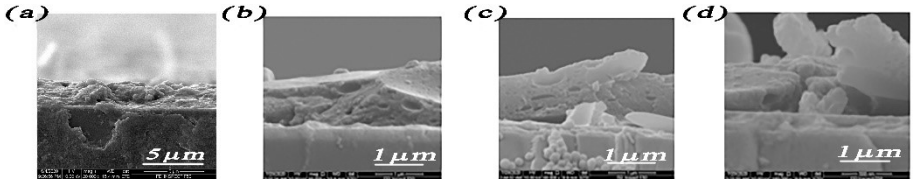

Figure S25 Cross-sectional FE-SEM photograph of (a)PI-1, (b)PI-2, (c)PI-3, and (d)PI-4 film electrode

6.

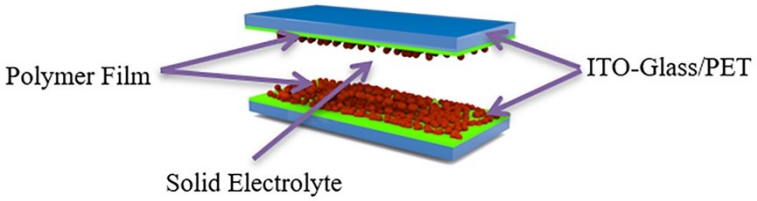

Figure S26 The structure of solid symmetrical electrochromic supercapacitor device

7.

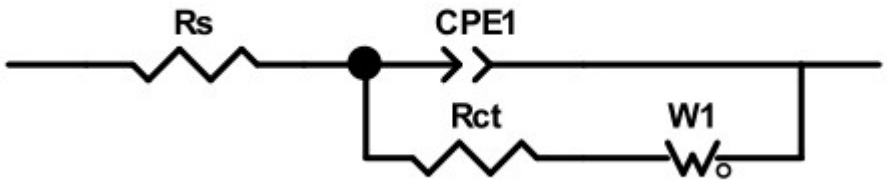

Figure S27 Equivalent circuit.

8. Calculation formula

Optical properties and energy level analysis

Firstly, the initial absorption value λ_{onset} of the polymer film in the ultraviolet spectrum should be known, and the band gap of the polymer can be obtained by the formula S(1)[4, 5].

$$Eg=1024/\lambda_{onset}\ ev \qquad S(1)$$

The test system was calibrated using ferrocene to give E(Fc/Fc+). The CV curve of the polymer over a wide range of voltages was tested and the initial oxidation potential Eox onset of the polymer was obtained. The HOMO/LUMO energy levels of the polymer can be obtained using the formulasS (2) and S(3) in combination with the Eg obtained previously[5].

$$HOMO=-[E_{oxonset}-E_{(Fc/Fc^{+})}+4.8]\ ev \qquad S(2)$$

$$LUMO= HOMO+E_g\ ev \qquad S(3)$$

Electrochromic property

First, the transmittance in the bleached state (T_b) of the polymer and the transmittance in the colored state (T_c) should be known. The optical conversion density ΔOD was obtained using the formula S(4). The unit charge amount Q_d of the

polymer was obtained by the chronoamperometry method, and the coloring efficiency CE can be calculated by the formula S(5). [6]

$$CE = \Delta OD / Q_d \quad S(4)$$

$$\Delta OD = \log(T_b / T_c) \quad S(5)$$

Electrochemical properties

The Area specific capacitance (C_{sA}) is calculated by the formula S(6). I_A is the current per unit area, $t_{discharge}$ is the discharge time of the material, A is the effective area of the electrode, and ΔV is the voltage window of the electrode. [7]

$$C_{sA} = I_A \cdot t_{discharge} / (A \cdot \triangle V) \quad S(6)$$

References:

(1) Oktem, G.; Balan, A.; Baran, D.; Toppare, L. Donor-acceptor type random copolymers for full visible light absorption. Chem Commun (Camb) 2011, 47, 3933-3935.

(2) Manceriu, L. M.; Rougier, A.; Duta, A. Comparative investigation of the Ti and Mo additives influence on the opto-electronic properties of the spray deposited WO3 thin films. J. Alloy. Compd. 2015, 630, 133-145.

(3) Li, H.; Chen, J.; Cui, M.; Cai, G.; Eh, A. L.; Lee, P. S.; Wang, H.; Zhang, Q.; Li, Y. Spray coated ultrathin films from aqueous tungsten molybdenum oxide nanoparticle ink for high contrast electrochromic applications. J. Mater. Chem. C 2016, 4, 33-38.

(4) Sun, Y.; Yang, Y.; Li, N.; Wang, M.; Chen, X.; Huang, S.; Yang, H. An “inverted load” strategy to fabricate interface-optimized flexible electrodes with superior electrochemical performance and ultrastability. Journal of materials

chemistry. C. 2020, 8, 11128-11137.

(5) Khan, A.; Usman, R.; Sayed, S. M.; Li, R.; Chen, H.; He, N. Supramolecular Design of Highly Efficient Two-Component Molecular Hybrids toward Structure and Emission Properties Tailoring. Cryst. Growth Des. 2019, 19, 2772-2778.

(6) Yoo, W.; Tsukamoto, T.; Kobayashi, S. Visible Light-Mediated Ullmann-Type C–N Coupling Reactions of Carbazole Derivatives and Aryl Iodides. Org. Lett. 2015, 17, 3640-3642.

(7) Afif, A.; Rahman, S. M.; Tasfiah Azad, A.; Zaini, J.; Islan, M. A.; Azad, A. K. Advanced materials and technologies for hybrid supercapacitors for energy storage – A review. Journal of Energy Storage 2019, 25, 100852.

(8) Yang, Y. L.; Lee, Y. H.; Lee, Y. P.; Chiang, C. J.; Hsu, F. Y.; Hsu, W. C.; Leung, M. K.; Wang, L.; Dai, C. A.; Ohta, Y.et al. Band gap tuning of narrow-polydispersity two-dimensional conductive polymers with electroactive side-chains. Journal of Polymer Science Part A: Polymer Chemistry 2014, 52, 1217-1227.